Structural Formation Studies of UV-Catalyzed Gels and Aerogels by Light Scattering

Arlon J. Hunt* and Michael R. Ayers

E. O. Lawrence Berkeley National Laboratory, University of California

Berkeley, California, USA 94720

The skeletal structure of aerogel is determined before, during, and after the gel is formed. Supercritical drying of aerogel largely preserves the pore structure that is determined near the time of gelation. To better understand these gel formation mechanisms we carried out measurements of the time evolution of light scattering in a series of gels prepared without conventional acid or base catalysis. Instead, ultraviolet light was used to catalyze the formation of silica gels made from the hydrolysis of tetraethylorthosilicate and partly prehydrolyzed tetraethylorthosilicate in ethanol. Time evolution of light scattering provides information regarding the rate and geometrical nature of the assembly of the primary silica particles formed in the sol. UV-catalyzed gels show volumetric growth typical of acid-catalyzed gels, except when UV exposure is discontinued at the gel point, where gels then show linear chain formation typical of base-catalyzed gels. Long term UV exposure leads to coarsening of the pore network, a decrease in the clarity of the aerogel, and an increase in the surface area of the aerogel. Additionally, UV exposure up to the gel point leads to increased crystallinity in the final aerogel.

Keywords: Aerogel, ultraviolet, sol-gel, light scattering

PACS Codes: 78.35; 81.05.R; 81.20.F; 61.80.B

1. Introduction.

As part of a program to study gelation in microgravity, we desired a method to accelerate the gelation of otherwise slow-gelling silica sols. The exposure of the sol to short-wavelength ultraviolet light is one means of accomplishing this. Short-wave UV is capable of cleaving many of the bonds found in alkoxide-based silica sols, such as, O-H, O-R, C-C, and C-H. However, common containers used to hold large sols are only partially transparent to wavelengths in the range of 200-250 nm. Therefore, only the curing effects of UV on thin-film SiO_2 gels has been previously reported [1, 2]. In these cases, UV exposure significantly increased the rate of gelation and the densification of the final xerogel. However, the effects of UV on the microstructure and porosity of large silica monoliths have not been explored.

Many detailed studies on the effects of pH on gel microstructure, porosity, and clarity have been reported [3-6]. There is a strong dependence on pH in both primary particle growth, and aggregation of particles and clusters into a gel. Additionally, even small amounts of acid or base catalysts greatly increase the rate of gelation in alkoxide-derived silica sols. As we desired to study sols with very long gel times, we examined the effects of UV on sols with no added catalyst, and report here the microstructural characteristics of the resulting gels and aerogels, as determined by light scattering, surface area measurements, TEM and x-ray diffraction.

2. Experimental Section.

Gel preparation utilized the following recipes; 0.083 mol precondensed TEOS ("Silbond H-5", Silbond Corp.)/1.3 mol anhydrous ethanol (UV grade)/0.83 mol H_2O ("Milli-Q" purity, 5MΩ resistance), and 0.083 mol TEOS (Aldrich Corp.)/1.0 mol anhydrous ethanol/0.83 mol H_2O. Fifty mL of each mixture was prepared and filtered through a 0.22-μm PTFE filter. The

mixtures were divided into 4 equal portions that were placed in 12 mm i.d. fused-silica tubes. The ends of each tube were sealed by PTFE plugs having viton o-rings.

Samples were exposed to ultraviolet light from two 15 Watt germicidal Hg-vapor lamps, in an enclosed light-box. The distance from the lamps to the samples was maintained at 10 cm. Samples were exposed for various lengths of time (T_{UV}), including, no exposure, 5 hours, T_{UV} = get time (T_{GEL}), and continuous exposure. After exposure was complete, samples were kept in the dark. The temperature of the samples in the light box were monitored periodically and found to be within 5 ºC of ambient conditions (~25 ºC).

The evolution of light scattering with time was measured at 532 nm and at 90º scattering angle, using the second harmonic of a Nd-YAG c.w. laser (Adlas DPY305II). Samples were removed from UV exposure at regular intervals and their scattering was measured and calibrated against a sealed CS_2 standard. Sample holders were indexed so that the identical sample orientation was measured at each interval.

When the scattering intensity stabilized with respect to time for all samples, the gels were removed from their holders and soaked in 30% H_2O/ethanol at pH 9.0 (NH_4OH) for 48 hours. Water was then removed from the gels by 4 soaks in 200 proof ethanol for 24 hours each. The aged alcogels were dried using standard CO_2-substitution/supercritical drying in a 300 mL Polaron critical-point dryer.

Single-point B.E.T. surface area measurements of the dried aerogels were obtained from the desorption isotherm of 30%N_2/He using a Quantasorb analyzer (Quantachrome, Inc.). UV-visible transmission spectra were obtained using an IBM 9410 spectrophotometer. X-ray diffraction powder patterns were collected on a Siemens Kristalloflex diffractometer using Cu

Kα radiation. TEM images were taken with a Topcon 002B microscope at 200 kV. Samples for TEM analyses were ground, suspended in acetone, and evaporated onto holey carbon-Cu grids.

3. Results and Discussion

Table 1 lists several physical characteristics of UV-catalyzed neutral silica sols, gels, and aerogels. With respect to gel time, two situations are apparent in these neutral sols. First, a significant decrease (~1/3 for precondensed silica and ~1/2 for TEOS sols) in the gel time is observed with continuos UV irradiation. This is consistent with a general increase in the rate of hydrolysis and condensation reactions leading to gelation. Additionally, TEOS sols show a shorter gel time in all cases. This does not appear to be related to UV exposure, as TEOS sols with $T_{UV} = 0$ show shorter get times, relative to all precondensed sols.

Table 1

Sample	**Precursor**	**T_{UV}** hours	**T_{GEL}** hours	**~Slope** (scat. vs. time)	**$\%T = A_* \exp(-Bt/\lambda^4)$** (A)	(B)	**Surface area** m^2/g
1	Precond.	0	720	6	0.5762	0.3260	480
2	Precond.	5 ($<<T_{GEL}$)	720	6	0.5570	0.3370	550
3	Precond.	250 ($= T_{GEL}$)	250	6, then 2	0.5724	0.3651	520
4	Precond.	1900 ($>>T_{GEL}$)	250	6	0.0554	0.3790	400
5	TEOS	0	96	6	0.9120	0.2900	530
6	TEOS	5 ($<<T_{GEL}$)	96	6	0.8146	0.2909	520
7	TEOS	27 ($= T_{GEL}$)	48	6, then 2	0.9254	0.2975	520
8	TEOS	260 ($>>T_{GEL}$)	48	6	0.9766	0.3029	510

Light scattering can be effectively used to monitor the formation of structure in evolving gel systems [7]. The greatest sensitivity for this technique occurs when features in the system

approximate the wavelength of light used in the measurement. For silica sols, visible light is most appropriate during the formation of larger clusters and their aggregation into a network gel [8]. The growth model of these clusters can be observed by plotting scattering intensity vs. time on a log-log scale, where spherical growth shows a slope of 6 and linear growth 2 [7]. Acid-catalyzed silica sols typically give a slope of 6, on this plot, while base catalyzed systems show a slope of 2. In this study, the neutral silica sols all show a slope of 6, consistent with the formation of weakly acidic Si-OH groups formed by the initial hydrolysis of Si-OR groups. One dramatic exception to this is seen when UV light exposure is ceased at T_{GEL}. In this case, the slope changes to 2 when UV is discontinued. There is no direct evidence for any cause of this change. However, as the aggregation of clusters during gelation is controlled by the surface potential of the clusters, it is possible that recombination products of photo-degraded species increase the surface charge on growing clusters, affecting their aggregation behavior. Figure 1 shows plots of light scattering vs. time for a series of gels made from precondensed silica.

Light scattering from internal features is the primary cause of poor clarity in dried silica aerogels. However, larger features, such as cracks, scratches, and bubbles, can also contribute to scattering. These two effects can be separated using the equation [7]:

$$T = A * exp\left[\frac{-B * t}{\lambda^4}\right] \quad (1)$$

where T is the % transmittance of an aerogel of thickness, *t,* at a wavelength, λ, and A and B are constants. Fitting the UV-visible spectrum of an aerogel to this equation gives A (the wavelength independent portion of light scattering, due to large features) and B (the wavelength dependent

portion, due to the internal gel structure). Values of A and B for the aerogels studied here appear in Table 1. All samples show an increase in B with longer UV exposure, indicating a coarsening of the internal structure of the gel due to UV light. A general decrease in surface area of the dried aerogels is also seen with prolonged UV exposure of the alcogel. Both of these effects indicate an enhancement of dissolution and reprecipitation reactions leading to both pore and particle growth.

Figure 2 shows TEM images for dried aerogels where $T_{UV} = T_{GEL}$, and $T_{UV} >> T_{GEL}$. Both show rather large primary particles (compared to base-catalyzed aerogels) an accord with the lower surface area of these aerogels. The image of the $T_{UV} = T_{GEL}$ sample shows a rather open structure as anticipated for a gel with a certain amount of linear cluster aggregation. The sample with $T_{UV} >> T_{GEL}$ shows a more dense compacted structure, consistent with spherical cluster growth. Both samples appeared predominantly amorphous to the electron beam. However, *some areas* of the sample $T_{UV} = T_{GEL}$ showed higher levers of crystallinity.

Figure 3 shows a TEM image of a portion of the $T_{UV} = T_{GEL}$ sample containing several <10 nm crystallites. Lattice planes can be seen in several locations (more can be seen with higher magnification). X-ray powder patterns, in Figure 4, show typical amorphous pattern for samples with $T_{UV} = 0$, $T_{UV} >> T_{GEL}$, and a standard 2-step acid-base catalyzed aerogel. However, the $T_{UV} = T_{GEL}$ sample shows a significantly different pattern, that is very broad (as expected for <10 nm particles), but similar to that found for dehydrated $H_2Si_4O_8$ precipitates [9]. Long-term aging of sol-gel sodium aluminosilcate gels has been shown to form increased numbers of crystallization nuclei compared to gels dried soon after gelation [10]. However, in our study, crystallinity is only observed when UV exposure was ceased at the gel point, and then only in a portion of the aerogel. It is likely that UV exposure forms dense SiO_2 particles by enhancement

of internal condensation reaction of surface -OH groups. These particles can then act as crystallization centers as particle growth very slowly continues after UV exposure is ceased.

4. Conclusions

Ultraviolet light during the wet stages of aerogel production can affect the final aerogel structure in several ways. Hydrolysis and condensation reactions are accelerated, leading to decreased gel times. Cluster-cluster aggregation is also affected by UV exposure, showing spherical cluster growth in most cases, but changing to linear aggregation when UV exposure is ceased at the gel point. Long term exposure during the aging process decreases the surface area, coarsens the internal microstructure of the gel, and forms crystallization nuclei within the gel. These factors can be attributed to an enhancement of -OH removal due to internal condensation reactions.

REFERENCES

[1] R.E. Van de Leest, App. Surface Sci. 86 (11995) 278.

[2] M. Niwano, K. Kinashi, K. Saito, N. Miyamoto, and K. Honma, J. Electrochem. Soc. 141 (1994) 1556.

[3] C.J. Brinker and G.W. Scherer, Sol-Gel Science (Academic Press, San Diego, 1990).

[4] W. Cao, and A.J. Hunt, J. Non-Cryst. Solids 176 (1994) 18.

[5] P.H. Tewari, A. J. Hunt, K.D. Lofftus, and J.G. Lieber M.R.S. Symp. Proc. 73 (1986) 195.

[6] R.E. Russo, A.J. Hunt, J Non-Cryst. Solids, 86 (1986) 219.

[7] A.J. Hunt, J Non-Cryst. Solids, *These proceedings.*

[8] K.D. Lofftus, K.V.S. Sastry, A.J. Hunt, Advanced Materials Proceedings (1990) 229.

[9] Lagaly, G., Beneke, K., Kammermeier, H., Z. Naturforsch., B: Anorg, Chem., Org. Chem 34B(5) (1979) 666.

[10] J.D. Cook, R.W. Thompson, Zeolites 8 (1988) 322.

FIGURE CAPTIONS

Fig. 1 Log-log plot of light scattering vs. time for precondensed silica sols. (●) $T_{UV} = 0$, (□)$T_{UV} << T_{GEL}$, (■)$T_{UV} = T_{GEL}$, (○)$T_{UV} >> T_{GEL}$. Lines show slopes of 2 and 6, arrows mark, gel points.

Fig. 2 TEM images of dried aerogels made from precondensed silica. Top, $T_{UV} >> T_{GEL}$, bottom, $T_{UV} = T_{GEL}$

Fig. 3 High magnification TEM image of a section of sample made from precondensed silica where, $T_{UV} = T_{GEL}$.

Fig. 4 X-ray powder patterns for aerogels made from precondensed silica sols. (a) 2-step acid-base catalyzed silica aerogel, (b) $T_{UV} >> T_{GEL}$ (c) $T_{UV} = 0$, (d)$T_{UV} = T_{GEL}$, (e). Crystal pattern from Ref. [8]

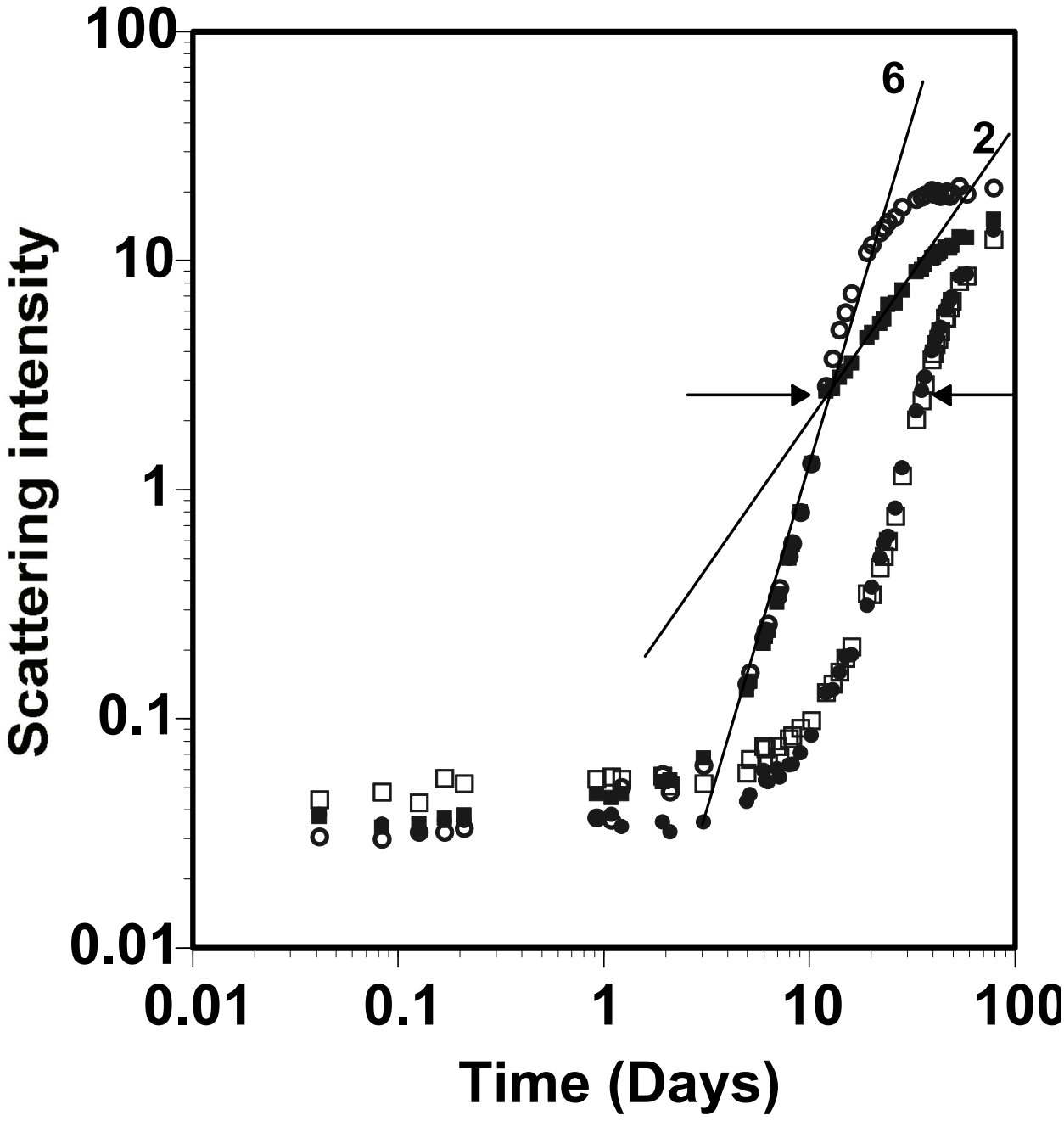

Figure 1 (AJ Hunt & MR Ayers)

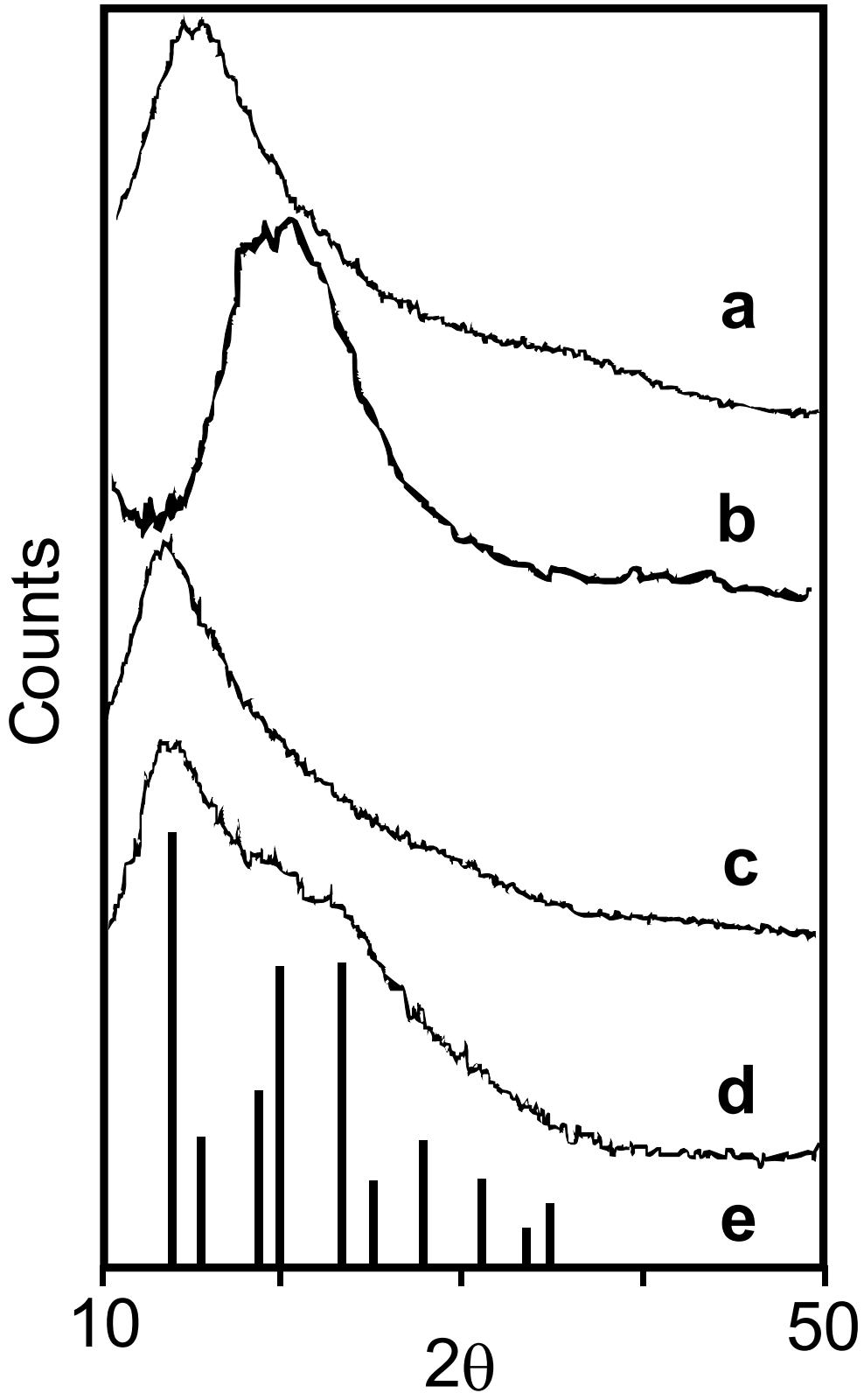

Figure 4 (AJ Hunt & MR Ayers)